CRYSTAL STRUCTURE, HIRSHFELD SURFACE ANALYSIS AND ENERGY FRAMEWORK STUDY OF THE NITRONE N-BENZYLIDENE-N-BUTYLAMINO-4-B-PYRIDYL-N-OXIDE

GERZON E. DELGADO [1,5], ASILOÉ J. MORA [1], ALI BAHSAS [2], VLADIMIR V. KOUSTNETZOV [3], CECILIA CHACÓN [4], JONATHAN CISTERNA [5], ALEJANDRO CÁRDENAS [6] AND IVÁN BRITO [5]*

[1]*Laboratorio de Cristalografía, Departamento de Química, Facultad de Ciencias, Universidad de Los Andes, Mérida 5101, Venezuela.*
[2]*Laboratorio de Resonancia Magnética Nuclear, Departamento de Química, Universidad de Los Andes, Mérida 5101, Venezuela.*
[3]*Laboratorio de Química Orgánica y Biomolecular, CMN, Universidad Industrial de Santander, Parque Tecnológico Guatiguará, Piedecuesta, Colombia.*
[4]*Cátedras Conacyt-Instituto Mexicano del Petróleo, Centro de Tecnologías para Exploración y Producción, Boca del Rio, México.*
[5]*Departamento de Química, Facultad de Ciencias Básicas, Universidad de Antofagasta, Avda. Universidad de Antofagasta 02800, Campus Coloso, Antofagasta 1240000, Chile.*
[6]*Departamento de Física, Facultad de Ciencias Básicas, Universidad de Antofagasta, Avda. Universidad de Antofagasta 02800, Campus Coloso, Antofagasta 1240000, Chile.*

ABSTRACT

The title compound, $C_{16}H_{16}N_2O$, a potential antiparasitic agent, crystallizes in the orthorhombic $Pca2_1$ space group with unit cell parameters a= 9.912(1) Å, b= 9.035(1) Å, c= 15.681(2) Å. The crystalline structure is stabilized by weak C---H···O and C--H···Cg(π) interactions among neighboring molecules producing an efficient packing with 66.0% of occupied space. The C--H···O hydrogen bond keeps the molecules linked into supramolecular chains propagating along the *a* axis direction with a graph-set notation C(4), which are reinforced by C--H···Cg(π) interactions. Hirshfeld surface analysis of the intermolecular contacts reveal that the most important contributions for the crystal packing are from H··H (55.2%) and H··C/C··H (27.1%) interactions. Energy framework calculations suggest that the contacts formed between molecules are slightly dispersive in nature.

Keywords: Nitrone, 1,3-dipolar cycloaddition, X-ray crystal structure, hydrogen bonds, Hirshfeld.

1. INTRODUCTION

The 1,3-dipolar cycloaddition reaction is one of the most useful reactions for the synthesis of heterocyclic compounds[1-4]. It provides one of his best tools for constructing five-membered rings. One of the most used molecules in this type of reactions are the nitrones, which are excellent building blocks in the preparation of novel heterocyclic structures by use of 1,3-dipolar cycloaddition, given that they represent a long-known and thoroughly investigated class of 1,3-dipoles[5-7]. Nitrones are rather flexible intermediates in organic synthesis and are used, for instance, in alkaloid synthesis[8], in the stereo-selective arrangement of synthetically important isoxazolidines oxadiazole[9] and in the synthesis of 2,6-disubstituted 4-hydroxypiperidines[10,11].

The most known procedures in the preparation of nitrones are the condensation of N-monosubstituted hydroxylamines with ketones or aldehydes[12], and the oxidation of secondary amines to their equivalent nitrones[13].

From the interest in studying the structural characterization of biologically active molecules[14-21], we report here the single-crystal X-ray diffraction study of the nitrone derivative N-benzylidene-N-butylamino-4-β-pyridyl-N-oxide, among a series of compounds with antiparasitic properties[10]. In order to understand the nature of the described non-covalent interactions in the supramolecular network of this material, a Hirshfeld surface analysis and energy framework study was performed[22,23].

2. EXPERIMENTAL SECTION

2.1 Synthesis

N-benzylidene-N-butylamino-4-β-pyridyl-N-oxide (**3**), was synthesized by a 1,3-dipolar cycloaddition reaction (Scheme 1) which is explained elsewhere[10]. Reagents and conditions: i) benzene, reflux, 6-10 h; ii) CH_2=$CHCH_2MgBr$/THF, r.t., 2 h; aq sat. NH_4Cl solution; iii) $Na_2WO_4.2H_2O$, 50% H_2O_2, acetone-H_2O, r.t., 2-4 d. Yield was 76%. X-ray quality crystals suitable for X-ray diffraction analysis were obtained from a solution of ethyl acetate after slow evaporation (m.p.: 130-132 ºC).

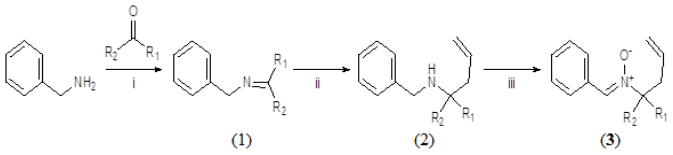

Scheme 1. Synthesis of N-benzylidene-N-butylamino-4-β-pyridyl-N-oxide (3). R_1= H, R_2= β-pyridyl.

2.2 FT-IR and NMR spectroscopic studies

The chemical structure of nitrone (**3**) was elucidated using FT-IR and ^{1}H-NMR. FT-IR spectra was obtained on a Perkin-Elmer 599B-FTIR spectrometer as KBr pellets, ^{1}H-NMR spectra was recorded on a Bruker Avance 400 model spectrometer in $CDCl_3$ solution.

IR υ_{max} cm^{-1}: 1639 (C=C), 1115, 923 (N→O), 1583 (C=N). ^{1}H NMR (400MHz, $CDCl_3$): δ = 1-H_{cis}: 5.01 (dd, J1-H_{cis},2= 9.2, J1,1= 1.5), 1-H_{trans}: 5.10 (dt, J1-H_{trans},2= 17.1, J1-H_{trans},3= 2.7); 2-H: 5.70 (m); 3-H_A,H_B: 3.22 (ddd), 2.64 (ddd), J3A,3B= 13.0, J3A,4 = 6.8, J3B,4= 5.9; 4-H: 4.88 (dd); N=CH: 7.50 (s); H_{arom}: 7.35-7.20 (m); R_1, R_2: 8.60 (d, α'-H), 8.50 (dd, α-H), 8.15 (t, β-H), 7.98 (dt, γ-H), $J_{\beta,\gamma}$= 7.7, $J_{\alpha,\beta}$= 6.5, $J_{\alpha',\gamma}$= 2.2, $J_{\alpha,\gamma}$= 1.6.

2.3 X-ray data collection and structure determination

A colourless rectangular crystal (0.63, 0.21, 0.13 mm) was used for data collection. Diffraction data were collected at 298(2) K by ω-scan technique on a Bruker Smart Apex II diffractometer equipped with graphite-monochromatized MoK_α radiation (λ = 0.71073 Å). The data were corrected for Lorentz-polarization and absorption effects. The structure was solved by direct methods using the SHELXS program[24] and refined by a full-matrix least-squares calculation on F^2 using SHELXL[25]. All H atoms were placed at calculated positions and treated using the riding model, with C-H distances of 0.97-0.98 A, and N-H distances of 0.86 A. The Uiso (H) parameters were fixed at 1.2Ueq (C, N) and 1.5Ueq (methyls). All geometrical calculations were done using the program Platon[25].

**Corresponding author email: gerzon@ula.ve*

Table 1 summarizes the crystal data, intensity data collection and refinement details for (**3**). CIF file containing complete information on the studied structure was deposited with CCDC, deposition number 1954958, and is freely available upon request from the following web site:

www.ccdc.cam.ac.uk/data_request/cif.

Table 1. Crystal data, data collection and structure refinement of (**3**).

Chemical formula	**$C_{16}H_{16}N_2O$**	**CCDC**	**1954958**
Formula weight	215.29	Radiation (MoKα)	λ = 0.71073 Å
Crystal system	Orthorhombic	θ range (°)	2.3-20.9
Space group	*Pca*2$_1$ (Nº29)	hkl range	-9, 9; -9, 5; -15, 13
a(Å)	9.912(1)	Reflections	
b(Å)	9.035(1)	Unique	1227
c(Å)	15.681(2)	Rint	0.027
V(Å^3)	1404.3(3)	With I > 2σ(I)	1101
Flack x	4(3)	Refinement method	Full-matrix least-squares F^2
Z	4	Number of parameters	172
dx (g cm^{-3})	1.193	R(F^2) [I > 2σ(I)]	0.0382
F(000)	536	wR(F^2) [I > 2σ(I)]	0.1088
μ(mm-1)	0.064	Goodness of fit on F^2	1.08
Crystal size (mm)	0.63 x 0.21 x 0.13	Max/min Δρ (e Å^{-3})	0.20/-0.23

2.4 X-ray powder diffraction

Powder X-ray diffraction (PXRD) study was carried out to check the purity and homogeneity of the bulk product of the title compound (3). The X-ray powder diffraction data was collected at room temperature 293(1) K, in θ/θ reflection mode using a Siemens D5005 diffractometer with CuKα radiation (λ= 1.5418 Å). The diffractometer was operated at 40 kV and 25 mA. The specimen was scanned from 5° to 65° 2θ, with a step size of 0.02° and counting time of 10 s per step. Quartz was used as an external standard.

2.5 Hirshfeld surfaces analysis

For the title compound, an analysis of the Hirshfeld surfaces[23] was performed with the aid of Crystal Explorer program[27]. The two-dimensional fingerprint plots were calculated for the crystal, as were the electrostatic potentials[28]. The electrostatic potentials were mapped on the Hirshfeld surfaces using the 3-21G basis set at the level of Hartree-Fock theory. Crystallographic information file (CIF) of (3) was used as input for the analysis. For the generation of fingerprint plots the bond lengths of hydrogen atoms involved in interactions were normalized to standard neutron values (C-H = 1.083 Å, N-H = 1.009 Å, O-H = 0.983 Å).

2.6 Energy framework study

The method of quantification of energy framework allow understand the topology of the overall interactions of molecules in a crystal[23]. This method allows calculate and compare the different energy components, i.e. repulsion (Erep), electric (Eele), dispersion (Edis), polarization (Epol) and total (Etot) energy based on the anisotropy of the topology of pairwise intermolecular interaction energies. Crystal Explorer program[27] was used to calculate the energy framework of the title compound by generating new wave functions using the DFT method under 3-21G basis set with exchange and potential functions (B3LYP) for a molecular cluster environment for a 1x1x1 unit cell. The thickness of the cylinder radius indicates the grade of interactions and is directly related to the energy magnitude and offers information about the stabilization of the crystal packing.

3. RESULTS AND DISCUSSION

3.1 Crystal and Molecular Structure

The nitrone derivative N-benzylidene-N-butylamino-4-β-pyridyl-N-oxide (3), $C_{16}H_{16}N_2O$, crystallizes in the orthorhombic space group *Pca*2$_1$. Figure 1 shows the molecular structure and the atom-labeling scheme of the title compound. Selected geometrical parameters are presented in Table 2. In the structure, all bond lengths and angles exhibit normal values for nitrone derivatives (Cambridge Structural Database, Version 5.41, March 2020)[29]. The bond lengths indicate double-bond character for the N1=C5 [1.292(5) Å] bond and single-bond character for the N1-C6 [1.523(5) Å] and N1-O1 [1.287(4) Å] bonds. The nitrone fragment Ph-CH=N(O)-C is planar to within 0.128(3) Å. It is almost perpendicular to the β-pyridyl substituent, with an O1-N1-C6-C7 torsion angle of 71.8(4)°, and forms a dihedral angle between the two aryl rings of 84.8 (2)º. Also, the nitrone fragment forms a dihedral angle between the phenyl ring and butyl group of 69.1(3)°. This is the same conformation as was previously observed in other compounds with nitrone fragments with refcodes KEMSIF[30], KEMSOL[30], VOJLUC[31] and JELQOJ[32], found in CSD database[29].

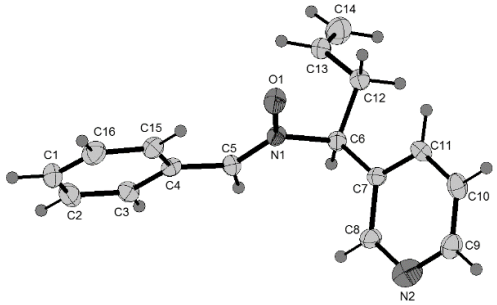

Figure 1. Atom numbering scheme of the title compound (3). Displacement ellipsoids are drawn at 25% probability level. H atoms are shown as spheres of arbitrary radii. The dotted line indicates the intramolecular hydrogen bond.

Table 2. Selected geometrical parameters (Å, º) for (3).

N1-O1	1.287(4)		N1-C5	1.292(5)
N1-C6	1.523(5)		N2-C8	1.383(6)
O1-N1-C5	125.9(3)		O1-N1-C6	114.8(3)
C5-N1-C6	119.3(3)		C8-N2-C9	119.6(4)
O1-N1-C5-C4	-2.1(6)		C6-N1-C5-C4	178.3(4)
O1-N1-C6-C7	71.8(4)		O1-N1-C6-C12	-55.5(4)

The crystalline structure of the title compound (**3**) is stabilized by one intramolecular and one intermolecular non-conventional hydrogen bonds. The geometrical parameters of these hydrogen bonds are summarized in Table 3 and Figure 2. The intramolecular C15--H15···O1 hydrogen bond generates an ring motif which can be described in graph-set notation as S(6)[32]. The intermolecular hydrogen bonds C5--H5···O1 (½+x, 1-y, z) keeps the molecules linked into supramolecular chains propagating along the *a* axis direction, with a graph-set notation C(4)[32] (Figure 2). Additional C--H···Cg(π) [C3--H3···Cg1 (½+x, 1-y, z) and C12--H12B···Cg2 (-x,1-y,-1/2+z) where Cg1and Cg2 are the centroid of the pyridyl and benzene rings], hydrogen bonds help to keep the chains together (see Figure 3).

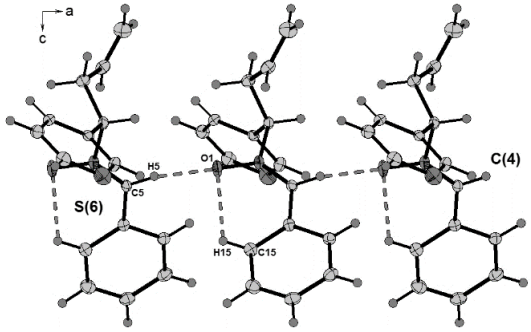

Figure 2. A partial view of the crystal packing in the *ca* plane, showing the hydrogen bonds contacts with graph-set S(6) and C(4).

Table 3. Parameters (Å, º) for short intermolecular contacts. (D-donor; A-acceptor; H-hydrogen). Cg1 and Cg2 represent the centroid of the pyridyl and benzene rings, respectively.

D--H···A	D--H	H···A	D···A	D--H···A
C5--H5···O1$^{(i)}$	0.930	2.360	3.233(5)	157
C15--H15···O1	0.930	2.380	2.932(5)	118
C3--H3···Cg1$^{(i)}$	0.930	2.900	-	-
C12--H12B···Cg2$^{(ii)}$	0.930	2.890	-	-

Symmetry codes: $^{(i)}$ ½+x, 1-y, z, $^{(ii)}$ -x,1-y,-1/2+z

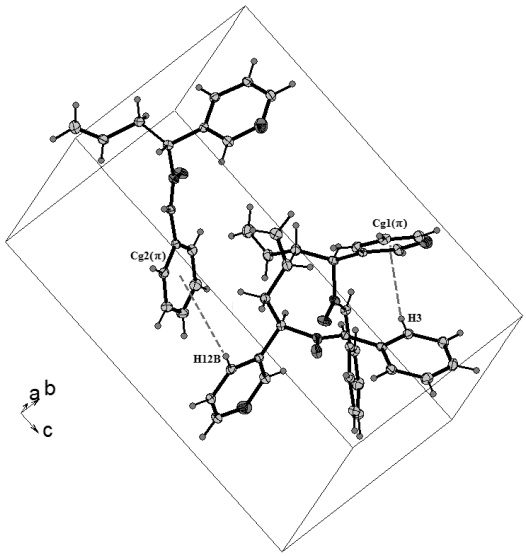

Figure 3. A partial view of the crystal packing for (**3**) showing the intermolecular weak C3--H3···Cg1$^{(i)}$ and C12--H12B···Cg2$^{(ii)}$ contacts.

3.2 Powder X-ray diffraction analysis

The X-ray powder pattern of the title compound (3) is shown in Figure 7a. The pattern was indexed in a monoclinic cell, which confirms the single-crystal results. In order to check the unit cell parameters, a Le Bail refinement[34] was carried out using the Fullprof program[35]. The Figure 7b shows a very good fit between the observed and calculated patterns. This results confirms the homogeneity of the sample and that the single crystals are representative of the bulk sample.

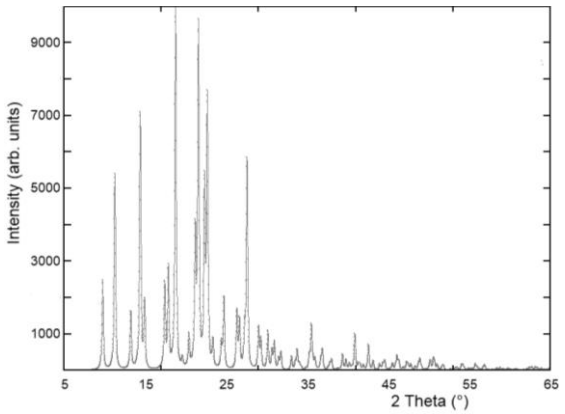

(a)

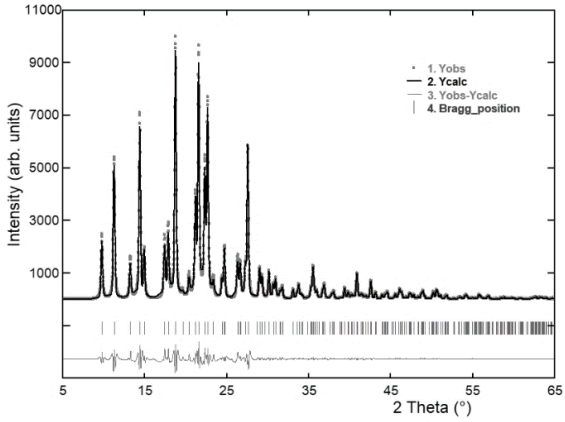

(b)

Figure 4. a) X-ray powder diffraction pattern of (**3**). b) Le Bail refinement of nitrone (**3**).

3.3 Hirshfeld surface analysis

A Hirshfeld surface analysis was conducted to verify the contributions of the different intermolecular interactions. This analysis was used to investigate the presence of hydrogen bonds and other weak intermolecular interactions in the crystal structure. The plots of the Hirshfeld surface confirms the presence of the non-covalent interaction described below (Figure 5).

In order to visualize and quantify the similarities and differences in intermolecular contacs across the crystal structure, the Hirshfeld surface analysis was made with complementary analyses such as shape index and curvedness surfaces The weak intermolecular interactions are mainly constituted by H···O, H···N, H···C and H···H, where the reciprocal contacts appear as a sharp needles for H···O, with $d_e + d_i \simeq 2.8$ Å (Figure 5e) , for H···N of the Hirshfeld surface and they appear as two diffuse wings, pointing at a distance greater than the van der Waals radii of N and H atoms with $d_e + d_i \simeq 3.1$ Å (Figure 5d) (di + de > 2.75 Å), with no significant contribution towards the crystal packing of the title molecule.

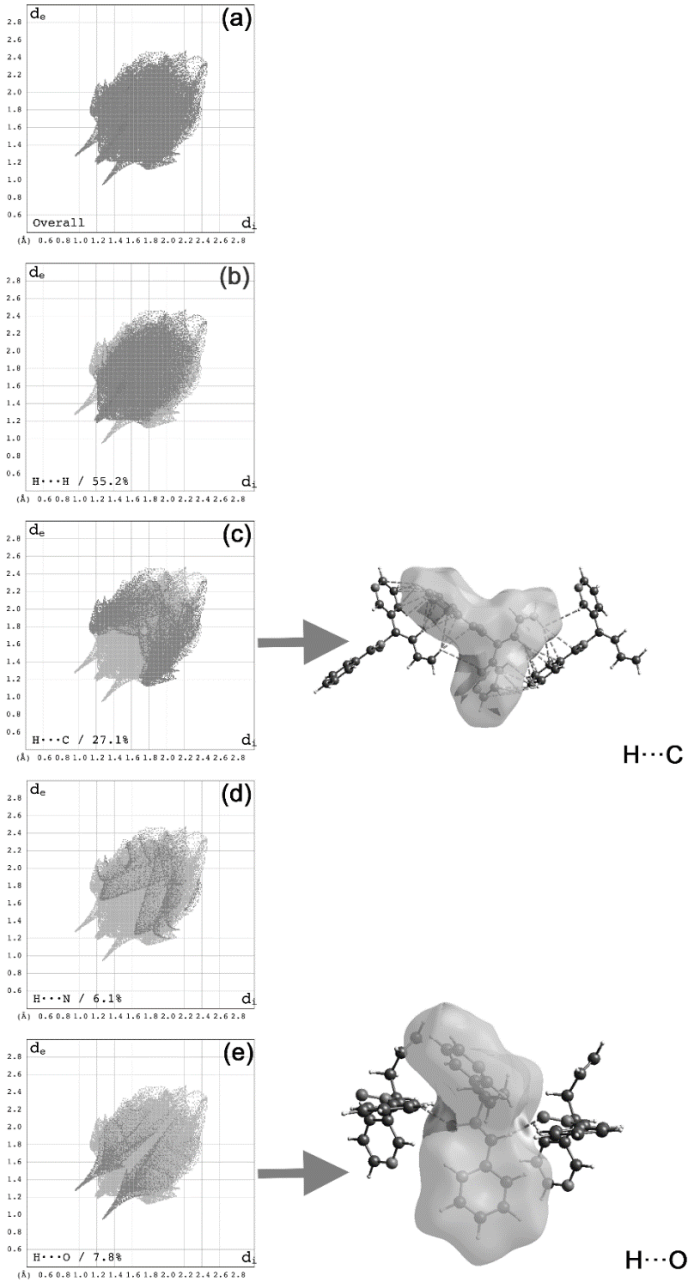

Figure 5. Hirshfeld surface of the title compound (left) and most representative contacts (right).

The, H···C as symmetrical thick wings with $d_e + d_i \simeq 3.0$ Å (Figure 5c) as consequence of H···π interaction, being one of major contribution in the crystal packing stabilization. The interatomic contacts of H···H have a majority of the all contribution in the surface generated (Figure 5b) showing a symmetrical sharp needle with $d_e + d_i \simeq 2.4$ Å, denoting H···H short contacts generating a significant effect over molecular packing in the crystal structure stabilization.

Shape index maps generated, allow to determine the presence of of H···π interaction over molecular structure, where the yellow-orange spots indicates the presence of this type of weak interaction over molecular structure where the interaction is stablished between the aromatic ring, pyridyl ring and nitrone fragments (Figure 6).

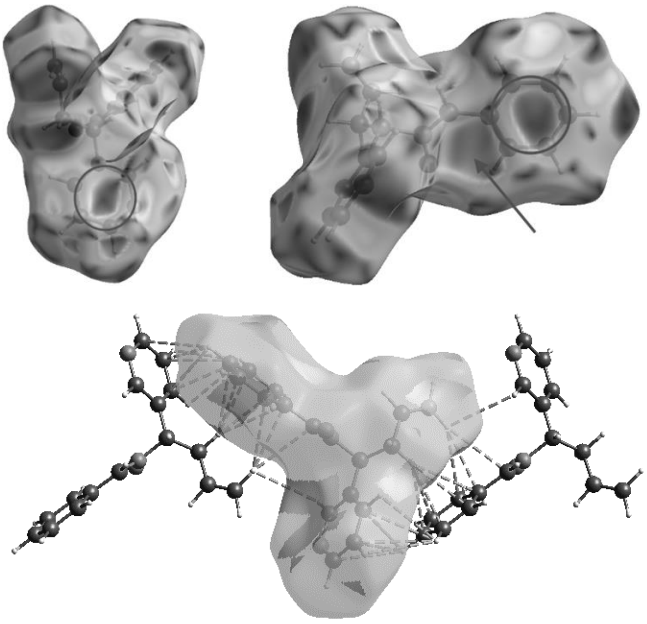

Figure 6. Shape index maps showing regions H···π interactions over the title compound (top) and interactions found in the crystal packing (bottom).

3.4 Energy Framework results

Energy framework was analysed to a better understanding of the packing of crystal structure and the supramolecular rearrangement. According to the tube direction, it can conclude that the formation of the framework is directed by the translational symmetry elements in each unit a long of *b* – axis due the stabilization of hydrogen bond interaction type directing the crystal structure layer by layer in the [110] plane disposing the molecular structure in a parallel setting, according to the electrostatic (E_{ele}).

The dispersion (E_{dis}) energy shows a 2D framework type cage as a component of the framework energy being more dominating than E_{ele} (see Figure 7). This rearrangement allows the formation of weak interactions in the crystal structure Such as H···π and classic hydrogen bond interactions, but not enough for the better stabilization of the framework. The low values of electrostatic total energy are attributed to the absence or few number of classical hydrogen bonds (see Table 4).

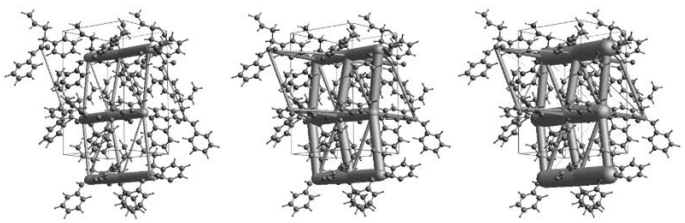

Figure 7. Energy framework diagrams for title compound viewed along [101], showing their respective type of energies.

Table 4. Energy framework detail of interaction with symmetry operations (symmop) and distances between molecular centroids (*R*) in Å.

N	Symop	R	E_ele	E_pol	E_dis	E_rep	E_tot
1	-x, -y, z+1/2	11.51	0.2	-0.1	-0.6	0.0	-0.4
1	-x+1/2, y, z+1/2	8.57	-5.1	-0.8	-11.5	3.6	-13.1
1	x+1/2, -y, z	4.96	-31.1	-12.1	-45.1	27.6	-57.8
1	x, y, z	9.91	-1.4	-0.1	-0.9	0.0	-2.3
1	-x, -y, z+1/2	7.98	-9.8	-2.4	-35.9	18.6	-28.8
1	x, y, z	9.03	-0.1	-3.2	-16.0	3.9	-13.5
1	-x, -y, z+1/2	14.75	-0.2	-0.0	-0.2	0.0	-0.4
1	-x+1/2, y, z+1/2	12.45	0.8	-0.4	-5.5	1.6	-3.1
1	x+1/2, -y, z	10.47	1.4	-1.6	-8.9	3.2	-5.0
1	x, y, z	15.68	-0.2	-0.0	-0.2	0.0	-0.3
1	x+1/2, -y, z	16.45	-0.2	-0.0	-0.1	0.0	-0.3
1	x, y, z	18.55	-0.1	-0.0	-0.0	0.0	-0.1
TOTAL			-45.8	-20.7	-124.9	58.5	-125.1

CONCLUSIONS

The nitron derivative N-benzylidene-N-butylamino-4-β-pyridyl-N-oxide has been synthetized from a 1,3-dipolar cycloaddition reaction and it crystal structure was determinate using X-ray single-crystal diffraction. The crystal packing is completely dominated by weak C---H···O and Cg(π) interactions among the neighboring molecules producing an efficient packing with 66.0 % of the occupied space. The intercontacts play a central crucial role in the stabilization of molecules in the crystal structure and were successfully verified with Hirshfeld surface analysis.

Two dimensional fingerprint plot calculations displayed the H···H and C···H pair of contacts that were the most significant interaction to the Hirshfeld surface. The three dimensional interaction energy analysis showed that, the dispersion energy frameworks Edis were dominant over classical electrostatic terms Eele.

ACKNOWLEDGEMENTS

This work was partially done into G.E. Delgado visit at the Universidad de Antofagasta, supported by MINEDUC-UA project, code ANT 1856. J. Cisterna, A. Cárdenas and I. Brito, thank to Universidad de Antofagasta for purchase license for the Cambridge Structural Database and for the financial support. G.E. Delgado thank to FONACIT (grant LAB-97000821).

REFERENCES

1. V. V. Kouznetsov, L. Vargas-Méndez, F. I. Zubkov, *Min. Rev. Org. Chem.* 13, 488 (2018).
2. L. Luna, L. Vargas-Méndez, V. V. Kouznetsov, *Org. Med. Chem. Int. J.* 7, 555708, (2018).
3. M. Acelas, V. V. Kouznetsov, A. R. Romero-Bohórquez, *Mol. Diversity*, 23, 183, (2019).
4. M. Breugst, R. Huisgen, H. U. Reissig, *Eur. J. Org. Chem*. 20, 2477, (2018).
5. R. A. Miranda-Quintana, P. W. Ayers, *Theor. Chem. Acc*. 135, 172, (2016).
6. R. A. Miranda-Quintana, M. Martínez-González, D. Hernández-Castillo, L. A. Montero-Cabrera, P. W. Ayers, C. Morell, *J. Mol. Model*. 23, 236, (2017).
7. A. Padwa, S. Bur, *Adv. Heterocycl. Chem*. 119, 241, (2016).
8. N. A. Bokach, M. L. Kuznetsov, V. Y. Kukushkin, *Coord. Chem. Rev*. 255, 2946, (2011).
9. K. V. Gothelf, K. A. Jørgensen, *Chem. Rev*. 98, 863-910 (1998).
10. A. Varlamov, V. V. Kouznetsov, F. Zubkov, A. Chernyshev, O. Shurupova, L. Y. Vargas, A. Palma, J. Rivero, A. J. Rosas-Romero, *Synthesis*, 29, 771, (2002).
11. V. V. Kouznetsov, J. Rivero, C. Ochoa, E. E. Stashenko, J. R. Martínez, C. Ochoa, D. Montero, J. J. Nogal, C. Fernández, S. Muelas, A. Gómez, A. Bahsas, J. Amaro-Luis, *Arch. Pharm. Chem. Life Sci.* 338, 32, (2005).

12. L. Hu, H. M. Martin, T. J. Strathmann, *Environ. Sci. Technol*. 44, 6416, (2010).
13. W. M Shi, X. P. Ma, G. F. Su, D. L. Mo, *Org. Chem. Front*. 3, 116, (2016).
14. I. Brito, J. Bórquez, D. Robledo, M. J. Simirgiotis, A. Cárdenas, *J. Chil. Chem. Soc*. 63, 4086, (2018).
15. A. M. Maharramov, G. Sh. Duruskari, G. Z. Mammadova, A. N. Khalilov, J. M. Aslanova, J. Cisterna, A. Cárdenas, I. Brito, *J. Chil. Chem. Soc*. 64, 4441, (2019).
16. A. R. Asgarova, A. N. Khalilov, I. Brito, A. M. Maharramov, N. G. Shikhaliyev, J. Cisterna, A. Cárdenas, A. V. Gurbanov, F. I. Zubkov, K. T. Mahmudov, *Acta Cryst*. *C*75, 342, (2019).
17. G. Mahmoudia, S. Rostamnia, G. Zaragoza, I. Brito, J. Cisterna, A. Cárdenas, *J. Chil. Chem. Soc*. (in press).
18. G. E. Delgado, E. Osal, A. J. Mora, T. González, A. Palma, A. Bahsas, *J. Struct. Chem*. 59, 1248, (2018).
19. G. E. Delgado, J. A. Henao, J. H. Quintana, H. M. Al-Maqtari, J. Jamalis, H. M. Sirat, *J. Struct. Chem*. 59, 1493, (2018).
20. L. E. Fernández, G. E. Delgado, L. V. Maturano, R. M. Tótaro, E. L. Varetti, *J. Mol. Struct*. 1168, 84, (2018).
21. G. E. Delgado, S. M. Liew, J. Jamalis, J. Cisterna, A. Cárdenas, I. Brito, *J. Mol. Struct*. 1210, 128044, (2020).
22. M. A. Spackman, P. G. Byrom, *Chem. Phys. Letters* 267, 215, (1997).
23. M. J. Turner, S. P. Thomas, M. W. Shi, D. Jayatilaka, M. A. Spackman, *Chem. Commun*. 51, 3735, (2015).
24. G. M. Sheldrick, *Acta Cryst. A*. 64, 112, (2008).
25. G. M. Sheldrick, *Acta Cryst. C*. 71, 3, (2015).
26. A. L. Spek, *J. Appl. Cryst*. 36, 7, (2003).
27. M. J. Turner, J. J. McKinnon, S. K. Wolff, S. K. Grimwood, P. R. Spackman, D. Jayatilaka, M. A. Spackman, Crystal Explorer 17.5. University of Western Australia, 2017.
28. M. A. Spackman, J. J. McKinnon, *CrystEngComm* 4, 378, (2002).
29. C. R. Groom, F. H. Allen, *Angew. Chem. Int. Ed*. 53, 662, (2014).
30. S. E. Denmark, J. I. Montgomery, *J. Org. Chem*. 71, 6211, (2006).
31. P. Merino, V. Mannucci, T. Tejero, *Eur. J. Org. Chem*. 23, 3943, (2008).
32. A. V. Churakov, P. V. Prikhodchenko, A. G. Medvedev, A. A. Mikhaylov, *Acta Cryst. E*, 73, 1666 (2017).
33. M. C. Etter, *Acc. Chem. Res*. 23, 120, (1990).
34. A. Le Bail, *Powder Diffr*. 20, 316, (2005)
35. J. Rodríguez-Carvajal, Fullprof version 7.20, Laboratoire Léon Brillouin (CEA-CNRS), France, 2019.